

The influence of misregistration between CT and SPECT images on the accuracy of CT-based attenuation correction of cardiac SPECT/CT imaging: Phantom and clinical studies

Leila Saleki^{1,2}, Pardis Ghafarian^{3,4}, Ahmad Bitarafan-Rajabi^{5,6},
Nahid Yaghoobi^{5,6}, Babak Fallahi⁷, Mohammad Reza Ay^{1,2}

¹Research Center for Molecular and Cellular Imaging, Tehran University of Medical Sciences, Tehran, Iran

²Department of Medical Physics and Biomedical Engineering, Tehran University of Medical Sciences, Tehran, Iran

³Chronic Respiratory Diseases Research Center, National Research Institute of Tuberculosis and Lung Diseases, Shahid Beheshti University of Medical Sciences, Tehran, Iran

⁴PET/CT and Cyclotron Center of Masih Daneshvari Hospital, Shahid Beheshti University of Medical Sciences, Tehran, Iran

⁵Cardiovascular Interventional Research Center, Department of Nuclear Medicine, Rajaei Cardiovascular, Medical, and Research Center, Iran University of Medical Sciences, Tehran, Iran

⁶Department of Nuclear Medicine, Rajaei Cardiovascular, Medical, and Research Center, Iran University of Medical Sciences, Tehran, Iran

⁷Research Center for Nuclear Medicine, Shariati Hospital, Tehran University of Medical Sciences, Tehran, Iran

(Received 2 July 2017, Revised 2 March 2019, Accepted 4 March 2019)

ABSTRACT

Introduction: Integration of single photon emission computed tomography (SPECT) and computed tomography (CT) scanners into SPECT/CT hybrid systems permit detection of coronary artery disease in myocardial perfusion imaging (MPI). Misregistration between CT and emission data can produce some errors in uptake value of SPECT images. The aim of this study was evaluate the influence of attenuation correction (AC) versus non-attenuation correction (NC) images and the effect of misregistration on all segments of SPECT images for quantitative and qualitative analysis.

Methods: 99 patients (45 males, 54 females) underwent stress/rest myocardial perfusion imaging (MPI) using ^{99m}Tc-MIBI were used in this study. We also utilized cardiac insert and lung insert in cylinder phantom. Phantom studies were performed with and without defect. The misregistration of all patient data was measured and variation in misregistration of our population was recorded. The effect of attenuation correction (AC) and non-attenuation correction (NC) images were also evaluated in both phantom and patient data. The CT images were shifted by ± 1 , ± 2 , ± 3 pixels along X-, Y- and Z-axis (Left/right, dorsal/ventral, cephalic/caudal) for both phantom and patient studies. Differences between misalignment data and misregistration correction images were also measured. Results displayed with 20 segments polar map analysis and illustration in standard orientations for cardiac tomographic images.

Results: In the patient population data, 1.5% were perfectly registered, 17% and 73% misaligned under 1 pixel and more than 1 pixel, respectively. AC of SPECT images showed increased uptake value in normal phantom and false positives findings were disappeared versus to NC images. In patient data, statistically significant variation were shown for the most segments before and after AC (P-value \leq 0.004) and also between AC of SPECT image and misregistration correction images (P-value \leq 0.048). Along X-axis, in 3 pixel shift in right direction, the percent of relative difference in lateral wall were 11.94% for mid anterolateral. Along Y-axis, the Ventral shift caused -15.9% changes in basal inferolateral and along Z-axis -8.59 % changes in apical anterolateral were also observed in caudal direction when 3 pixel shifts were used.

Conclusion: This study showed that CT-based attenuation correction of cardiac images in hybrid SPECT/CT is important to improve image quality. Misalignment in caudal, cephalad, ventral and right direction introduced significant variation even in 1 pixel shift. It is important to apply misregistration correction even in small misalignment routinely in clinical myocardial perfusion imaging.

Key words: Cardiac SPECT/CT; Attenuation correction; Misregistration artifact; Image registration; Myocardial perfusion imaging

Iran J Nucl Med 2019;27(2):63-72

Published: July, 2019

<http://irjnm.tums.ac.ir>

Corresponding author: Dr Pardis Ghafarian, Chronic Respiratory Diseases Research Center, National Research Institute of Tuberculosis and Lung Diseases (NRITLD), Shahid Beheshti University of Medical Sciences, Tehran, Iran.
E-mail: pardis.ghafarian@sbmu.ac.ir

INTRODUCTION

Myocardial perfusion imaging (MPI) with single photon emission computed tomography (SPECT) is a successful imaging method for the detection of coronary artery disease (CAD) in daily clinical routine [1, 2]. However, non-uniform tissues attenuation in the thorax, specially lung, diaphragm and breast tissue can be the source of false positive result and artifacts in myocardial perfusion SPECT image [3]. Today's, attenuation map are obtained with computed tomography (CT) for SPECT emission data. Advantages of the CT scan for attenuation correction (AC) consist of lower noise, faster acquisition, higher quality, higher photon flux, no decay of transmission source and improved resolution [4, 5]. It is clear that CT imaging in hybrid system can also increase the likelihood of misregistration between CT and emission data [6], increasing the patient absorbed dose [7-9] and increasing CT artifact to emission data [10-12].

Huang et al. demonstrated that attenuation correction in post stress MPI scan by SPECT/CT can be possibly more helpful in men than women [13]. It was shown that using attenuation correction can lead to improve quantitative accuracy [14]. Goetze et al. stated that radioactivity distribution can be significantly changed when registration correction was performed for MPI [5]. Goetze et al. revealed that registration is important to prevent misregistration artifact in cardiac perfusion imaging [15]. The purpose of this study was to assess the clinical usefulness of CT based attenuation correction in myocardial perfusion imaging and to determine the role of misregistration on cardiac images interpretation by patient and phantom study. In the first step, the difference between uptake value for NC and AC images were assessed in both phantom and

patient studies. In the next step, we evaluated the amplitude of misregistration in our patient population. Then, for consideration of misregistration influence on uptake value for all segments of cardiac SPECT, misregistrations in different directions were manually created and the importance of misregistration correction for AC images was evaluated.

METHODS

Phantom study

The phantom studies were performed using a cylinder phantom (an inside diameter of 21.6cm), cardiac insert (model ECT/CAR/I; with Solid/Fillable Defect Set) and lung insert. The chest body phantom consists of lung inserted that filled with water (soft tissue equivalent material) and the cardiac phantom was placed inside the water-filled cylindrical phantom at the position of the human heart. The cardiac insert include a ventricle and myocardial chamber (Figure 1).

In this study, two strategies were applied for phantom studies. In the first, the cardiac phantom was simply filled with 8mCi of Tc-99m solution. In the second, we added two solid defects in cardiac phantom: (i) in mid anterolateral segment with 2 cm height, 5 mm wall thickness, and (ii) in basal inferoseptal segment with 2 cm height, 1 cm wall thickness.

Patient population

The study was consist of 99 patients (45 men and 54 women; mean age \pm SD; 56.87 \pm 10.34y, mean body mass index \pm SD; 28.53 \pm 5.78 kg/(m)²) who underwent stress-rest myocardial perfusion imaging that injected with ^{99m}Tc-MIBI.

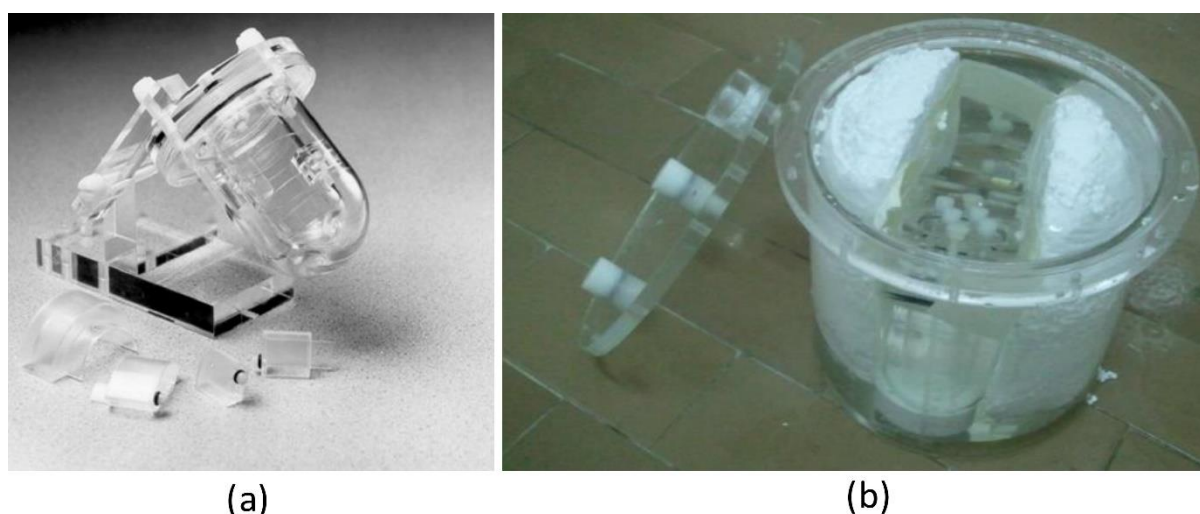


Fig 1. Photographs of phantoms used in this study; a) Cardiac Insert™, Model ECT/CAR/I, b) cylinder chest phantom with lung and cardiac insert.

Data acquisition and processing

Myocardial perfusion imaging was acquired using Infinia Hawkeye-4 SPECT/CT camera (dual head, GE Healthcare) equipped with low-energy, high-resolution, parallel-hole collimator and with a 37×37cm field of view and zoom factor of 1.5. Each patient underwent a two-day stress-rest ^{99m}Tc-MIBI protocol. Patients were permitted to breathe normally during both the SPECT and the CT scans, in the supine position with their arm above the head.

SPECT imaging was performed with the following specifications for both phantom and patient studies: each rectangular detector was in position 90° and rotated from the left anterior oblique to the left posterior oblique positions; 60 frames of 3° (30 steps over a 180° scan) and 20 s per projection. A 64 × 64 projection matrix of 5.9-mm² pixel size was used. For emission data, 20% energy window was set and centered at 140 keV. The CT scanner was a low dose multi-slice (4 slices) helical CT with 140-kV and 2.5-mA of current tube and pitch of 1.9:1 with slice thickness 5mm. SPECT data were reconstructed by Ordered-Subsets Expectation Maximization (OSEM) with 2 iterations and 10 subsets. Reconstructed images were smoothed by use of a Butterworth filter with a critical frequency of 0.35 and power of 10.0 and processed on a Xeleris workstation (GE Healthcare). Attenuation correction (AC) and non-attenuation correction (NC) images were displayed in 4DM-SPECT software on the standard orientations for cardiac tomographic images as short axis, horizontal long axis and vertical long axis for visual analysis and twenty-segment polar map for semi-quantitative analysis. Radiotracer uptake intensity was regionally normalized to maximum cardiac value in each segment, set for polar map display (range; 0%-100%).

Quantification and correction of misregistration

Correction of the misregistration between SPECT and CT images was done manually with the manufacturer's software (ACQC tool; GE Healthcare). CT images shifted in X, Y and Z directions to obtain the best cardiac edges according to SPECT images. In this step, Euclidian distance of

mismatched was calculated by $\sqrt{(x^2 + y^2 + z^2)}$. Maximum normalized count in 20 segments for non-corrected and attenuation-corrected images before and after reregistration was compared. To determine the influence of amount of misregistration, the CT images were shifted by ±1, ±2, ±3 pixels (1 pixel=5.9 mm) in the X, Y and Z-axis (left/right, dorsal/ventral, cephalic/caudal) according to SPECT images. Maximum normalized count difference was also compared between each shifted image and reregistered image.

Statistical analysis

Data were reported as mean ± SD. Paired-sample t-test was used for comparing data between the NC images and AC images, before and after misregistration correction. General Linear Model test was also used to determine the influence of any pixel shift of CT images on the SPECT images. P-value ≤ 0.05 was considered statistically significant.

RESULTS

The SPECT images of cardiac insert phantom without any defects were illustrated in Figure 2 in NC and AC images. It is obvious that the artifactual inferior defect in NC cardiac phantom image was eliminated in attenuation correction of SPECT image.

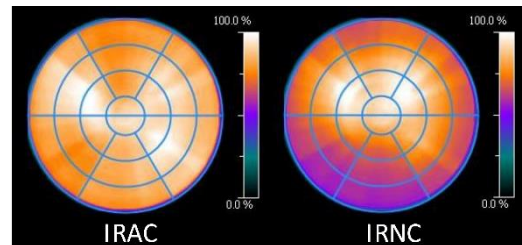


Fig 1. The influence of attenuation correction on uptake value in SPECT images of cardiac phantom without any defects. Left, iteratively reconstructed attenuation-corrected (IRAC), right, iteratively reconstructed non-attenuation-corrected (IRNC).

Figure 3 showed the effect of two defects in NC and AC on the polar maps of SPECT images. After AC the summed rest score (SRS) value varied from 14 to 5 and showed significantly improvement in real uptake value.

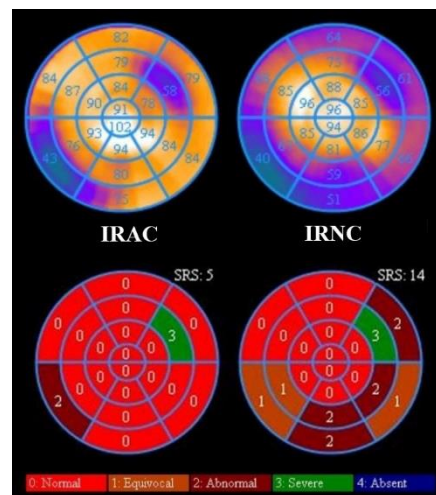


Fig 3. The influence of attenuation correction on uptake value in SPECT images of cardiac phantom with two defects. Left, iteratively reconstructed attenuation-corrected (IRAC), right, iteratively reconstructed non-attenuation-corrected (IRNC).

In our patient population except 3 studies (1.5%) which were perfectly registered, the other studies showed misalignment. 35 studies (17%) misaligned under 1 pixel, 144 studies (73%) misaligned more than 1 pixel, included 13 studies (6.5 %) misaligned between 1-2 pixels and 3 studies (1.5%) more than 3 pixels. It should be clear that, least and most misregistration error occurred in Y- direction (-0.60 ± 3.64 mm) with a range of 0-30.8 mm and in x-direction (6.41 ± 3.64 mm) with a range of 0-20.2 mm, respectively. Moreover, misregistration more than 1 pixel occurred 67%, 11% and 20%, in the X-, Y- and Z- axis, respectively. Figure 4 shows a representative example from a stress myocardial perfusion image of woman patient in which a lateral defect was created after AC that was reduced after correction for misregistration.

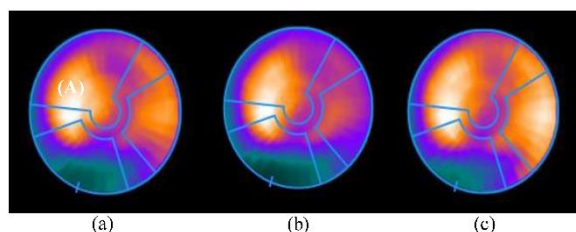


Fig 4. The polar map of the stress myocardial perfusion for a typical woman patient. (a), Non-attenuation correction, (b), Attenuation Correction and (c) Attenuation correction image after correction for misregistration.

In our patient study, significant differences between AC and NC for maximum normalized percentage of all polar map segments were shown except in apical inferoseptal, basal anterolateral, and apical inferolateral segments and also between AC and misregistration correction images except anteroapical, apical anterior, basal anterolateral and mid inferior segments (Table 1). For accurate evaluation of the misalignment in various directions on regional radiotracer uptakes in SPECT images, we produced a systematic misregistration by shifting the CT image relative to SPECT image (± 1 , ± 2 , ± 3 pixels along X, Y and Z axis). With regard to statistical analysis, it was obvious that in our patient study, misalignment for dorsal and left directions introduced the less variation (Table 2). The percent of relative difference in all segments of polar map between misregistration correction image and shifted images along X, Y and Z axis were illustrated in Figures 5, 6 and 7, respectively. Along X-axis, the most severe differences caused by right and left shift in segments of the lateral wall. In 3 pixel shift in right direction, the percent of relative difference in lateral wall were -9.12% for basal inferolateral, -10.00% for basal anterolateral, -10.71% for mid inferolateral, 11.94% for midanterolateral, -10.23% for apical inferolateral and -9.77% for apical anterolateral (Figure 5). Along Y-axis, the most

variation was seen in Ventral shift that caused -15.9% changes in basal inferolateral, -10.6% change in mid inferolateral, -10.8% changes in basal anterolateral and -10.2% changes in mid anterolateral segments for 3 pixel shift (Figure 6). Along Z-axis -8.59 % change in apicalanterolateral, -8.18% variation in mid anterolateral and -7.79% change in basal anterolateral were also observed in caudal direction when 3 pixel shift has occurred (Figure 7).

DISCUSSION

This study revealed that although AC is essential to improve image quality and quantification measurements in SPECT/CT imaging, misregistration error due to global, cardiac and respiratory motion can produce some errors in interpretation of cardiac images in hybrid imaging corresponding to previous studies [16, 17]. It seems that misregistration correction can be important for AC images in hybrid imaging in routine clinical myocardial perfusion imaging. Several phantom and patient studies demonstrated an improvement in SPECT image quality with attenuation correction [18-21]. Nevertheless, misalignment between the emission and transmission scans can create some artifacts in the MPI [5, 6]. We observed, even 1 pixel shift (5.9 mm) can create significant errors in uptake value of SPECT images. Apostolopoulos et al. showed that clinical interpretation of MPI in SPECT/CT varied in 11%, 18% and 73% situations when registration carried for misalignment <1 pixel, 1-2 pixels and ≥ 2 pixels, respectively [22]. Quantitative and qualitative phantom results confirmed the accuracy of the AC in myocardial SPECT imaging that was increased by using CT based attenuation correction, in line with the findings by Patton et al. [20]. After AC of phantom image, we observed an accurate severity and proper location of the solid defects while non-attenuation corrected images showed false defects in other segments and increase of uptake value in location of the solid defect. Huang et al. also stated that using attenuation correction for TI-201 MPI introduced significant useful diagnostic information especially for obese and male patients due to enhance of specificity [23]. In our patient population, significant variation in uptake value were observed for the most segments before and after AC (P -value ≤ 0.004) and also in the AC SPECT images when compared to misregistration correction images (P -value ≤ 0.048). Our findings indicated that using registration correction seems to be important in clinical interoperation of MPI in SPECT/CT even in small misalignment, although the amplitude and misalignment direction are also important factors in accurate interoperation which is in line with the pervious investigation [22].

Table 1: Comparison of the Maximum Normalized Percentage in 20 segments of polar map for all patients in this study for NC, AC images before and after misregistration correction.

Segment	IRNC	IRAC	MD ⁺	P ⁺	IRAC-MC	MD [*]	P [*]	MD [‡]	P [‡]
Anteroapical	84.28 ± 10.23	79.14 ± 7.99	-5.14	<0.001	79.29 ± 8.02	-4.99	<0.001	0.15	NS
Inferoapical	82.22 ± 11.01	77.62 ± 8.88	-4.61	<0.001	78.16 ± 8.75	-4.07	<0.001	0.54	0.048
Basal Anterior	72.05 ± 7.75	73.33 ± 6.87	1.28	0.002	72.30 ± 6.77	0.25	NS	-1.03	<0.001
Mid Anterior	79.23 ± 8.84	80.35 ± 7.31	1.12	0.004	79.77 ± 7.11	0.54	NS	-0.58	0.004
Apical Anterior	80.65 ± 9.73	77.05 ± 7.43	-3.60	<0.001	76.85 ± 7.42	-3.80	<0.001	-0.20	NS
Basal Anteroseptal	59.21 ± 9.65	61.17 ± 9.70	1.95	<0.001	59.84 ± 9.73	0.63	<0.001	-1.32	0.001
Basal Inferoseptal	58.25 ± 11.29	67.62 ± 11.60	9.37	<0.001	66.35 ± 11.51	8.10	<0.001	-1.27	<0.001
Mid-Anteroseptal	84.22 ± 7.89	88.34 ± 6.18	4.12	<0.001	87.19 ± 6.68	2.96	<0.001	-1.16	<0.001
Mid Inferoseptal	81.03 ± 8.45	89.34 ± 5.86	8.32	<0.001	88.27 ± 6.07	7.25	<0.001	-1.07	<0.001
Apical Anteroseptal	85.88 ± 8.36	84.86 ± 7.03	-1.02	0.003	84.17 ± 7.03	-1.71	<0.001	-0.69	<0.001
Apical Inferoseptal	88.75 ± 7.98	88.58 ± 5.88	-0.17	NS	87.99 ± 5.96	-0.76	NS	-0.59	0.001
Basal Inferolateral	73.46 ± 9.71	80.05 ± 9.37	6.59	<0.001	80.95 ± 9.69	7.49	<0.001	0.90	0.004
Basal Anterolateral	78.25 ± 7.64	78.29 ± 7.68	0.04	NS	78.66 ± 7.57	0.40	NS	0.36	NS
Mid Inferolateral	81.40 ± 9.01	86.18 ± 8.47	4.78	<0.001	87.42 ± 8.11	6.02	<0.001	1.24	<0.001
Mid Anterolateral	87.95 ± 7.57	85.56 ± 8.14	-1.39	<0.002	87.65 ± 7.16	-0.30	NS	1.09	<0.001
Apical Inferolateral	79.43 ± 8.26	79.88 ± 7.39	0.45	NS	81.35 ± 7.14	1.92	<0.001	1.47	<0.001
Apical Anterolateral	83.35 ± 9.60	80.20 ± 7.82	-3.16	<0.001	81.26 ± 7.70	-2.09	<0.001	1.07	<0.001
Basal Inferior	63.17 ± 12.41	77.03 ± 12.75	13.86	<0.001	76.41 ± 12.57	13.24	<0.001	-0.62	<0.001
Mid Inferior	72.07 ± 11.66	83.48 ± 9.82	11.42	<0.001	83.44 ± 9.28	11.37	<0.001	-0.05	NS
Apical Inferior	75.30 ± 10.22	77.26 ± 7.98	1.96	<0.001	77.83 ± 7.66	2.54	<0.001	0.58	0.002

⁺Comparison of IRNC and IRAC

^{*}Comparison of IRNC and IRAC-MC

[‡]Comparison of IRAC and IRAC-MC

IRNC = iteratively reconstructed non-attenuation-corrected

IRAC = iteratively reconstructed attenuation-corrected

IRAC-MC = iteratively reconstructed attenuation-corrected study after correction for misregistration

MD = mean difference

NS= non-significant

S= significant

Table 2: Statistical comparison between perfect alignment of ACimage and misalignment images with various pixel shifts.

Segment	P Value																	
	Magnitude of misregistration on -x direction (Right)			Magnitude of misregistration on X direction (Left)			Magnitude of misregistration on -Y direction (Ventral)			Magnitude of misregistration on Y direction(Dorsal)			Magnitude of misregistration on -Z direction (Caudal)			Magnitude of misregistration on Z direction (Cephalic)		
	3	2	1	1	2	3	3	2	1	1	2	3	3	2	1	1	2	3
Anteroapical	NS	NS	NS	NS	NS	NS	0.003	0.010	0.026	NS	NS	NS	<0.001	<0.001	0.033	0.045	NS	0.020
Inferoapical	NS	NS	NS	NS	NS	NS	0.018	0.039	NS	NS	NS	NS	NS	0.002	<0.001	<0.001	<0.001	<0.001
Basal Anterior	0.030	NS	NS	NS	NS	NS	0.040	NS	NS	NS	NS	NS	<0.001	<0.001	<0.001	0.044	0.002	<0.001
Mid Anterior	0.003	NS	NS	NS	NS	NS	NS	NS	NS	NS	NS	NS	<0.001	<0.001	<0.001	<0.001	<0.001	<0.001
Apical Anterior	NS	NS	NS	NS	NS	NS	0.007	0.009	0.023	NS	NS	NS	<0.001	<0.001	<0.001	<0.001	<0.001	<0.001
Basal Anteroseptal	NS	NS	NS	NS	NS	NS	0.013	NS	NS	NS	NS	NS	<0.001	<0.001	0.003	NS	NS	0.018
Basal Inferoseptal	NS	NS	NS	NS	NS	NS	NS	NS	NS	NS	NS	NS	0.044	<0.001	0.024	NS	NS	NS
Mid Anteroseptal	0.029	0.045	NS	NS	NS	NS	0.042	0.046	NS	NS	NS	NS	<0.001	<0.001	0.003	NS	NS	NS
Mid Inferoseptal	NS	NS	NS	NS	NS	NS	NS	NS	NS	NS	NS	NS	NS	NS	NS	NS	0.003	<0.001
Apical Anteroseptal	0.005	0.004	0.009	NS	NS	NS	<0.001	<0.001	0.002	NS	NS	NS	<0.001	0.011	NS	NS	NS	0.016
Apical Inferoseptal	0.035	0.033	0.044	NS	NS	NS	0.001	0.005	0.030	NS	NS	0.016	<0.001	<0.001	<0.001	<0.001	<0.001	<0.001
Basal Inferolateral	<0.001	<0.001	0.037	NS	NS	0.041	<0.001	<0.001	0.001	NS	0.005	<0.001	0.001	<0.001	NS	NS	NS	NS
Basal Anterolateral	<0.001	<0.001	0.006	NS	0.004	<0.001	<0.001	<0.001	0.008	NS	0.003	<0.001	<0.001	<0.001	<0.001	<0.001	<0.001	<0.001
Mid Inferolateral	<0.001	<0.001	0.015	NS	0.049	0.032	<0.001	<0.001	0.033	NS	NS	0.017	0.002	NS	NS	NS	NS	0.026
Mid Anterolateral	<0.001	<0.001	0.003	0.037	0.008	0.004	<0.001	<0.001	0.044	NS	0.031	0.003	<0.001	<0.001	<0.001	<0.001	<0.001	<0.001
Apical Inferolateral	<0.001	<0.001	0.026	NS	NS	0.039	0.001	0.020	NS	NS	NS	NS	0.004	NS	<0.001	NS	<0.001	<0.001
Apical Anterolateral	<0.001	<0.001	0.039	NS	0.026	0.017	0.021	NS	NS	NS	NS	NS	<0.001	<0.001	<0.001	<0.001	<0.001	0.034
Basal Inferior	0.038	NS	NS	NS	NS	NS	<0.001	<0.001	<0.001	NS	NS	NS	NS	<0.001	NS	NS	NS	NS
Mid Inferior	NS	NS	NS	NS	NS	NS	0.018	NS	NS	NS	NS	NS	<0.001	<0.001	0.005	<0.001	<0.001	<0.001
Apical Inferior	NS	NS	NS	NS	NS	NS	NS	NS	NS	NS	NS	NS	<0.001	<0.001	<0.001	<0.001	<0.001	<0.001

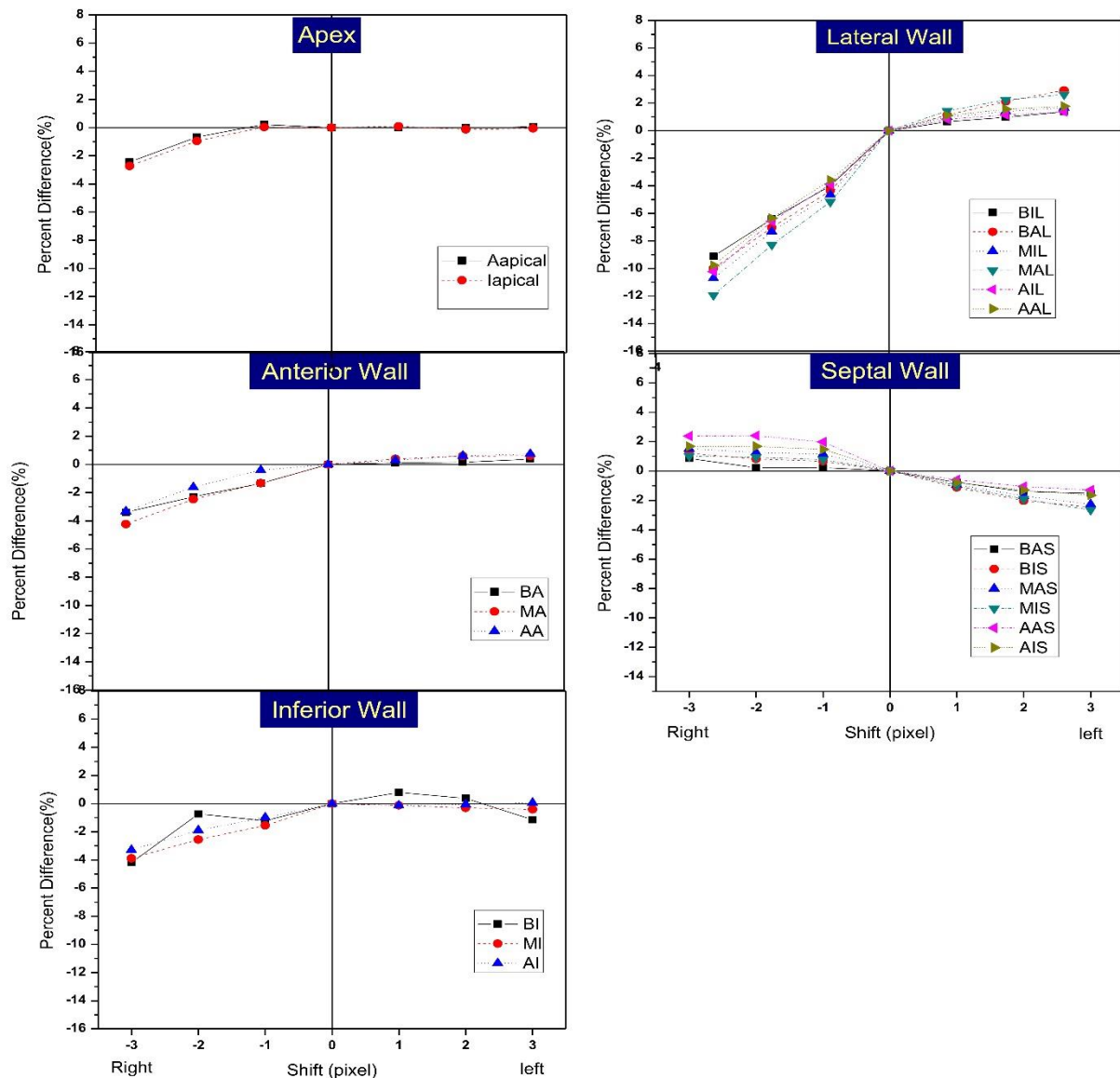


Fig 5. Percent of relative difference in polar map segment between misregistration correction of SPECT image and shifted imaged by ± 1 , ± 2 , ± 3 pixels in X-direction.

Phantom image without any defects illustrated the observed error of uptake value was increased with increasing of pixel shifts (score 3, 2, 1 for 3 pixel shift versus to score 2, 1 for 2 pixel shift although score 0 was correct value) in left and right direction (data are not shown), that were in agreement with previous study [17]. For our patient data, misregistration in X-axis demonstrated serious effect in lateral wall (right and left direction), anterior and inferior wall for right direction. It was obvious that significant variation was seen in right compared with left direction. Polycarpou et al. revealed that artifact in MPI of SPECT/CT can be decreased when using both respiratory motion correction and attenuation correction [24]. It seems interesting that inferior and anterior segment of left ventricle in myocardial walls showed the most

effect when respiratory motion correction was applied. All segments in misalignment along Y-axis showed significant effect for uptake value with more impact in lateral wall in ventral direction. In general, ventral direction revealed more variation versus dorsal direction in all segments of polar map. Along Z-axis, all segments illustrated the significant effect which is in line with the findings of the previous study [17] with more impact for lateral and anterior wall in caudal direction even for 1 pixel shift. This behavior can be due to the respiratory motion. It should be mentioned that, along Z-axis the significant effect can be observed as compared to X and Y axis. In some shifted image, we observed the decreased of uptake value compared with alignment image due to interference of lung tissue in AC images.

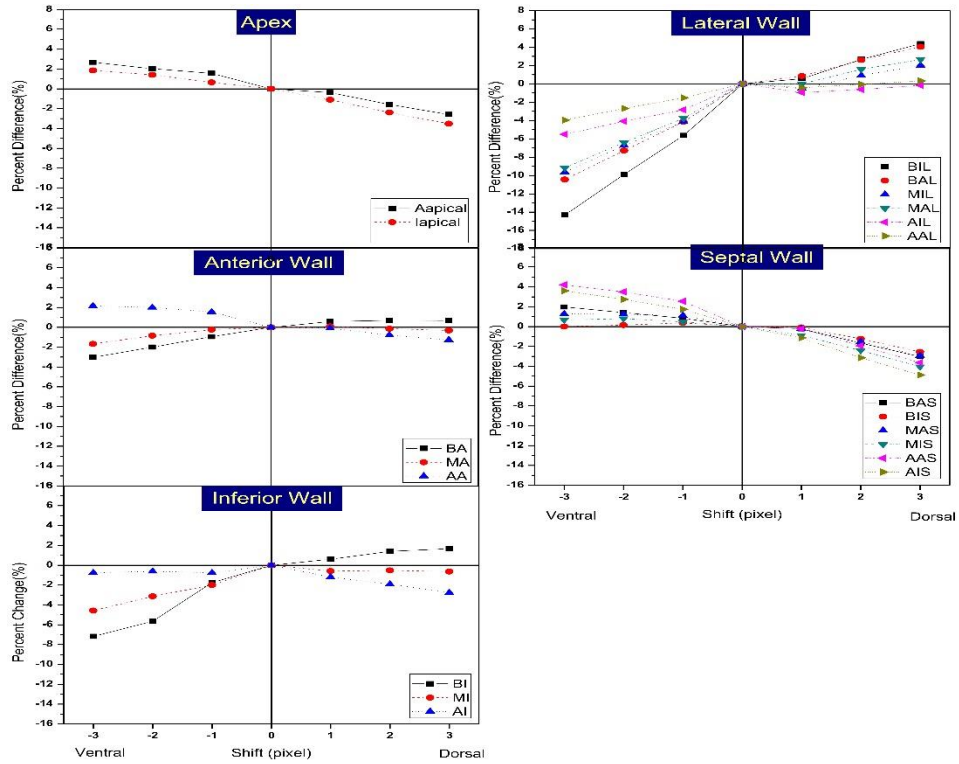


Fig 6. Percent of relative difference in polar map segment between misregistration correction of SPECT image and shifted imaged by $\pm 1, \pm 2, \pm 3$ pixels in Y-direction.

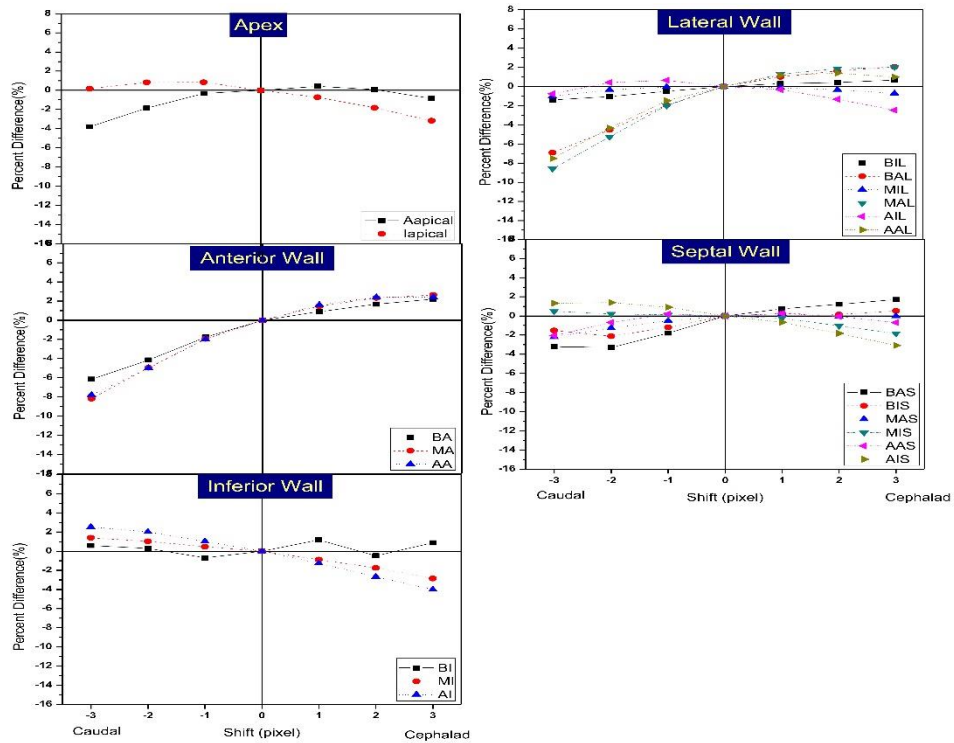


Fig 7. Percent of relative difference in polar map segment between misregistration correction of SPECT image and shifted imaged by $\pm 1, \pm 2, \pm 3$ pixels in Z-direction.

Although diaphragm and muscles can generate higher uptake value compared with aligned image, it should be noted that, Patchett et al. demonstrated that visual evaluation of coronary artery calcium in CTAC can be useful when MPI of SPECT/CT was done for improvement of diagnostic information [25]. The effect of misregistration in various segments of cardiac images in our data had some variation compared with Kennedy et al. [26] likely due to different in polar map application (5-segment versus to 20-segment). Our investigation had some limitation; 1) manual shifting of the CT images for misregistration correction by physician which was time consuming, 2) the results were not classified according to patient's weight and gender.

CONCLUSION

Although CT-based attenuation correction of cardiac images in hybrid SPECT/CT imaging introduced some benefit in image quality but misregistration error can also produce some error in interpretation. Misregistration correction is vital for accurate quantification even in the presence of small misalignment. Misalignment in caudal, cephalad, ventral and right direction introduced significant variation even in 1 pixel shift with less variation being observed in left and dorsal direction. In general misregistration can produce both underestimation and overestimation of uptake value however the impact of this behavior depends on the direction and degree of misalignment.

Acknowledgments

This work was supported by Tehran University of Medical Sciences under grant number 30849.

REFERENCES

- Hachamovitch R. Prognostic characterization of patients with mild coronary artery disease with myocardial perfusion single photon emission computed tomography: validation of an outcomes-based strategy. *J Nucl Cardiol.* 1998 Jan-Feb;5(1):90-5.
- Russell RR 3rd, Zaret BL. Nuclear cardiology: present and future. *Curr Probl Cardiol.* 2006 Sep;31(9):557-629.
- Zaidi H, Hasegawa BH. Attenuation correction strategies in emission tomography. quantitative analysis in nuclear medicine imaging. Springer; 2006. p. 167-204.
- Bybel B, Brunken RC, DiFilippo FP, Neumann DR, Wu G, Cerqueira MD. SPECT/CT imaging: clinical utility of an emerging technology. *Radiographics.* 2008 Jul-Aug;28(4):1097-113.
- Goetze S, Brown TL, Lavelly WC, Zhang Z, Bengel FM. Attenuation correction in myocardial perfusion SPECT/CT: effects of misregistration and value of reregistration. *J Nucl Med.* 2007 Jul;48(7):1090-5.
- Geramifar P, Zafarghandi MS, Ghafarian P, Rahmim A, Ay MR. Respiratory-induced errors in tumor quantification and delineation in CT attenuation-corrected PET images: effects of tumor size, tumor location, and respiratory trace: a simulation study using the 4D XCAT phantom. *Mol Imaging Biol.* 2013 Dec;15(6):655-65.
- Ay M, Shahriari M, Sarkar S, Ghafarian P. Measurement of organ dose in abdomen-pelvis CT exam as a function of mA, KV and scanner type by Monte Carlo method. *Int J Radiat Res.* 2004;1(4):187-194
- Ay MR, Mehranian A, Maleki A, Ghadiri H, Ghafarian P, Zaidi H. Experimental assessment of the influence of beam hardening filters on image quality and patient dose in volumetric 64-slice X-ray CT scanners. *Phys Med.* 2013 May;29(3):249-60.
- Ghafarian P, Aghamiri SM, Ay MR, Fallahi B, Rahmim A, Schindler TH, Ratib O, Zaidi H. Coronary calcium score scan-based attenuation correction in cardiovascular PET imaging. *Nucl Med Commun.* 2010 Sep;31(9):780-7.
- Ay MR, Mehranian A, Abdoli M, Ghafarian P, Zaidi H. Qualitative and quantitative assessment of metal artifacts arising from implantable cardiac pacing devices in oncological PET/CT studies: a phantom study. *Mol Imaging Biol.* 2011 Dec;13(6):1077-87.
- Etemadi Z, Ghafarian P, Bitarafan-Rajabi A, Malek H, Rahmim A, Ay MR. Is correction for metallic artefacts mandatory in cardiac SPECT/CT imaging in the presence of pacemaker and implantable cardioverter defibrillator leads? *Iran J Nucl Med.* 2018;26(1):35-46.
- Ghafarian P, Aghamiri SM, Ay MR, Rahmim A, Schindler TH, Ratib O, Zaidi H. Is metal artefact reduction mandatory in cardiac PET/CT imaging in the presence of pacemaker and implantable cardioverter defibrillator leads? *Eur J Nucl Med Mol Imaging.* 2011 Feb;38(2):252-62.
- Huang R, Li F, Zhao Z, Liu B, Ou X, Tian R, Li L. Hybrid SPECT/CT for attenuation correction of stress myocardial perfusion imaging. *Clin Nucl Med.* 2011 May;36(5):344-9.
- Gerdekoohi SK, Vosoughi N, Tanha K, Assadi M, Ghafarian P, Rahmim A, Ay MR. Implementation of absolute quantification in small-animal SPECT imaging: Phantom and animal studies. *J Appl Clin Med Phys.* 2017 Jul;18(4):215-223.
- Goetze S, Wahl RL. Prevalence of misregistration between SPECT and CT for attenuation-corrected myocardial perfusion SPECT. *J Nucl Cardiol.* 2007 Apr;14(2):200-6.
- Ghafarian P, Ay M. The influence of PET and CT misalignment due to respiratory motion on the cardiac PET/CT imaging: a simulation study. *Front Biomed Technol.* 2015;1(4).
- Ghafarian P, Ay MR, Fard-Esfahani A, Rahmim A, Zaidi H. Quantification of PET and CT misalignment errors due to bulk motion in cardiac PET/CT imaging: phantom and clinical studies. *Front Biomed Technol.* 2014;1(3).
- Fricke E, Fricke H, Weise R, Kammeier A, Hagedorn R, Lotz N, Lindner O, Tschoepe D, Burchert W. Attenuation correction of myocardial SPECT perfusion images with low-dose CT: evaluation of the method by comparison with perfusion PET. *J Nucl Med.* 2005 May;46(5):736-44.
- Heller GV, Bateman TM, Johnson LL, Cullom SJ, Case JA, Galt JR, Garcia EV, Haddock K, Moutray KL, Poston C, Botvinick EH, Fish MB, Follansbee WP, Hayes S, Iskandrian AE, Mahmarijan JJ, Vandekerckhove W. Clinical value of attenuation correction in stress-only Tc-99m sestamibi

- SPECT imaging. *J Nucl Cardiol.* 2004 May-Jun;11(3):273-81.
20. Patton JA, Turkington TG. SPECT/CT physical principles and attenuation correction. *J Nucl Med Technol.* 2008 Mar;36(1):1-10.
 21. Pazhenkottil AP, Ghadri JR, Nkoulou RN, Wolfrum M, Buechel RR, Küest SM, Husmann L, Herzog BA, Gaemperli O, Kaufmann PA. Improved outcome prediction by SPECT myocardial perfusion imaging after CT attenuation correction. *J Nucl Med.* 2011 Feb;52(2):196-200.
 22. Apostolopoulos DJ, Gašowska M, Savvopoulos CA, Skouras T, Spyridonidis T, Andrejczuk A, Vassilakos PJ. The impact of transmission-emission misregistration on the interpretation of SPET/CT myocardial perfusion studies and the value of misregistration correction. *Hell J Nucl Med.* 2015 May-Aug;18(2):114-21.
 23. Huang JY, Yen RF, Lee WC, Huang CK, Hsu PY, Cheng MF, Lu CC, Lin YH, Chien KL, Wu YW. Improved diagnostic accuracy of thallium-201 myocardial perfusion single-photon emission computed tomography with CT attenuation correction. *J Nucl Cardiol.* 2018 Feb 26. doi: 10.1007/s12350-018-1230-y.
 24. Polycarpou I, Chrysanthou-Baustert I, Demetriadou O, Parpottas Y, Panagidis C, Marsden PK, Livieratos L. Impact of respiratory motion correction on SPECT myocardial perfusion imaging using a mechanically moving phantom assembly with variable cardiac defects. *J Nucl Cardiol.* 2017 Aug;24(4):1216-1225.
 25. Patchett ND, Pawar S, Miller EJ. Visual identification of coronary calcifications on attenuation correction CT improves diagnostic accuracy of SPECT/CT myocardial perfusion imaging. *J Nucl Cardiol.* 2017;24(2):711-20.
 26. Kennedy JA, Israel O, Frenkel A. Directions and magnitudes of misregistration of CT attenuation-corrected myocardial perfusion studies: incidence, impact on image quality, and guidance for reregistration. *J Nucl Med.* 2009 Sep;50(9):1471-8.